Learning Bad from
Good with PKA Dynamics

PKA Dynamics in a *Drosophila* Learning Center: Coincidence Detection by Rutabaga Adenylyl Cyclase and Spatial Regulation by Dunce Phosphodiesterase

Nicolas Gervasi,[1] Paul Tchénio,[1,2] and Thomas Preat[1,*]
[1]Genes and Dynamics of Memory Systems, Neurobiology Unit, Ecole Supérieure de Physique et Chimie Industrielle, CNRS, 10 rue Vauquelin, 75005 Paris, France
[2]Nanospectroscopy, Université Paris-Sud, CNRS UPR 3321, Batiment 505, Campus d'Orsay, 91400 Orsay, France
*Correspondence: thomas.preat@espci.fr
DOI 10.1016/j.neuron.2010.01.014

SUMMARY

The dynamics of PKA activity in the olfactory learning and memory center, the mushroom bodies (MBs), are still poorly understood. We addressed this issue in vivo using a PKA FRET probe. Application of dopamine, the main neuromodulator involved in aversive learning, resulted in PKA activation specifically in the vertical lobe, whereas octopamine, involved in appetitive learning, stimulated PKA in all MB lobes. Strikingly, MB lobes were homogeneously activated by dopamine in the learning mutant *dunce*, showing that Dunce phosphodiesterase plays a major role in the spatial regulation of cAMP dynamics. Furthermore, costimulation with acetylcholine and either dopamine or octopamine led to a synergistic activation of PKA in the MBs that depends on Rutabaga adenylyl cyclase. Our results suggest that Rutabaga acts as a coincidence detector and demonstrate the existence of subcellular domains of PKA activity that could underlie the functional specialization of MB lobes in aversive and appetitive learning.

INTRODUCTION

During classical conditioning, a conditioned stimulus (CS) is linked temporally with a positive or negative unconditioned stimulus (US). Following association of the two stimuli, the CS alone will elicit a conditioned response characteristic of the US. *Drosophila melanogaster* can be classically conditioned both aversively and appetitively, by association of an odorant with electric shock or sugar (Keene and Waddell, 2007). This system represents a powerful model with which to investigate the neuronal mechanisms underlying learning and memory, not least because of the wide range of molecular genetic and imaging tools available (Gerber et al., 2004; Liu and Davis, 2006; Keene and Waddell, 2007).

The mushroom body (MB) was the first brain region to be shown to play a role in *Drosophila* olfactory learning (Heisenberg et al., 1985). Flies with ablated MB structures are completely defective in associative learning (de Belle and Heisenberg, 1994). Moreover, MB synaptic output is involved in both appetitive and aversive memory processing (Dubnau et al., 2001; McGuire et al., 2003; Schwaerzel et al., 2003; Isabel et al., 2004; Krashes et al., 2007; Krashes and Waddell, 2008). In adult *Drosophila*, the MBs consist of approximately 2500 intrinsic neurons per brain hemisphere, named the Kenyon cells. Kenyon cell bodies are located in the dorsal posterior part of the brain, and project dendrites to form a neuropil field called the calyx. Adult Kenyon cells may be classified into three major types based on their axonal projection configuration: γ neurons, which form a single medial lobe, α/β neurons, whose axons branch to form a vertical (α) and a medial (β) lobe, and α'/β' neurons, which also form a vertical (α') and a medial (β') lobe (Crittenden et al., 1998).

The first two *Drosophila* genes identified in blind screens for learning and memory mutants correspond to two components of the cyclic AMP (cAMP) cascade. *Dunce* (*dnc*) encodes a cAMP-specific phosphodiesterase (PDE), whereas *rutabaga* (*rut*) encodes a type I Ca^{2+}/calmodulin-stimulated adenylate cyclase (AC) (Dudai et al., 1976; Byers et al., 1981; Livingstone et al., 1984). Several studies in other systems indicate that this type of AC may serve as a molecular site of convergence between the US and the CS (Abrams and Kandel, 1988; Wu et al., 1995). Thus, type I AC may act as a coincidence detector that integrates Ca^{2+} influx (resulting from the CS) and G protein activation (resulting from the US-induced binding of a neuromodulator to its G protein-coupled receptor). Biochemical studies have shown that AC activation increases the local concentration of cAMP, leading to cAMP-dependent protein kinase A (PKA) activation through dissociation of the cAMP-binding regulatory subunit from the catalytic subunit (Taylor et al., 1990). In *Drosophila*, strong modifications of the activity of the major PKA catalytic subunit (DCO) impair olfactory memory (Drain et al., 1991; Skoulakis et al., 1993; Yamazaki et al., 2007), whereas a mild decrease in DCO activity enhances a specific form of long-lasting memory, known as anesthesia-resistant memory (Horiuchi et al., 2008).

Consistent with their role in learning and memory, Rut, Dnc, and DCO proteins are all preferentially expressed in MB neurons, albeit with slightly different expression patterns (Nighorn et al., 1991; Han et al., 1992; Skoulakis et al., 1993). The distinct gene expression profiles and morphologies of the individual

lobes suggest that they may have distinct functions. This has been confirmed by functional studies showing that (1) Rut AC is required in the α/β and γ MB lobes for normal learning and short-term memory (Zars et al., 2000; Akalal et al., 2006), (2) Rut is sufficient in α/β neurons to sustain partial long-term memory (Blum et al., 2009), (3) an early memory trace is formed in α'/β' MB neurons (Krashes et al., 2007; Wang et al., 2008), (4) vertical lobes are involved in aversive long-term memory (Pascual and Preat, 2001), and (5) a long-term aversive memory trace forms within the α branch of the α/β MB neurons (Yu et al., 2006). In addition, memory acquisition and consolidation require neurotransmission from α'/β' MB neurons (Krashes et al., 2007).

These results indicate that the MBs and the cAMP/PKA pathway are critically important for olfactory learning and memory. However, the spatiotemporal dynamics of cAMP/PKA signaling in the *Drosophila* MBs are poorly understood. Evidence currently suggests that dopaminergic neurons represent the reinforcing substrate of an aversive US (Claridge-Chang et al., 2009), whereas the reinforcing stimulus of an appetitive US is signaled through octopaminergic neurons (Schwaerzel et al., 2003; Schroll et al., 2006). Dopaminergic and octopaminergic neurons innervate wide areas of the brain including the MBs (Nassel and Elekes, 1992; Riemensperger et al., 2005; Sinakevitch and Strausfeld, 2006; Busch et al., 2009). However, it remains unclear how the different components of this signaling pathway interact dynamically in vivo and, in particular, in which MB compartment they operate. We therefore do not know how the numerous cAMP/PKA-related proteins interact with each other during learning and memorization, or even whether they are important in the same sets of MB neurons.

In the present study, we used in vivo multiphoton imaging to measure the dynamics of PKA responses to dopamine and octopamine in the MB neurons of living flies. We performed real-time measurements of PKA activity using the genetically encoded FRET probe AKAR2 (Zhang et al., 2001, 2005). The AKAR2 probe is based on a phosphothreonine-binding domain derived from yeast (FHA1) and an optimized PKA substrate domain. When phosphorylated by PKA, the substrate domain interacts with the binding pocket of the FHA1 domain, increasing the FRET between two GFP variants CFP and citrine. The reporter is a substrate for endogenous PKA and therefore simultaneously reports the activities of endogenous PKA and its opposing phosphatases (Zhang et al., 2005).

Our work with AKAR2 in the *Drosophila* MBs indicates that this sensor is functional and suitable for detection of PKA signaling in living flies. We present data that address important questions about the dynamics of PKA in MB neurons and integration of neuromodulatory signals. In particular, we show that MB dendrites and axons integrate cAMP/PKA stimulation with different efficiencies and time courses. This activity is modified in *rut* and *dnc* learning and memory mutants. Furthermore, we demonstrate that dopaminergic stimulation, which represents the aversive US, leads to activation of PKA specifically in the α lobes, whereas octopamine activates PKA in all MB lobes. We show that dopamine-induced PKA activity is restricted to the α lobes by Dnc PDE. Finally, we show that Rut AC potentiates PKA activation when dopamine or octopamine stimulations are temporally paired with increased intracellular calcium.

RESULTS

AKAR2 Expression Does Not Alter MB Development and Physiology

We generated recombinant flies carrying insertions of the AKAR2 gene, and used the Gal4/UAS system to drive expression of the probe in MB neurons (see Experimental Procedures). Before analyzing PKA dynamics in vivo, we needed to verify that AKAR2 expression does not affect brain development and neuronal morphology. We expressed the AKAR2 probe in MB neurons both during development and in the adult using the driver 238Y-Gal4. This driver has a broad expression and is not restricted to MB neurons (Yang et al., 1995; Connolly et al., 1996). As expected, *238Y-Gal4/UAS-AKAR2* flies display CFP and YFP fluorescence in MB cell bodies, calyces, and all MB lobes (Figure 1C). At this level of resolution, no defects in MB structure are detected following AKAR2 expression, in contrast to a previously described sensor, PKA-GFP, whose expression led to developmental abnormalities (Lissandron et al., 2007).

We tested whether the physiology of MB neurons is affected by AKAR2 expression or the 238Y driver. *238Y-Gal4/UAS-AKAR2* flies were trained with the aversive or appetitive olfactory conditioning protocols (Tully et al., 1994; Pascual and Preat, 2001; Krashes and Waddell, 2008; Colomb et al., 2009). Both aversive and appetitive short-term and long-term memory were found to be normal (see Figure S1 available online). Thus, AKAR2 expression did not disrupt the ability of MB neurons to mediate olfactory learning and memory.

Recording PKA Dynamics in the MBs of Living Flies

Two-photon microscopy is particularly suitable for noninvasive fluorescence imaging of tissue explants and living animals, as it provides both reduced photodamage outside the focal volume and increased depth penetration (hundreds of microns) compared with conventional confocal microscopy. We first verified by two-photon imaging that the AKAR2 sensor is able to detect changes of PKA activity in vivo after direct stimulation of the cAMP-generating enzyme AC. The dose-response curve of the effect of forskolin (Figure 1B), an activator of most forms of AC (de Souza et al., 1983), shows a clear increase in the YFP/CFP emission ratio in all the MB compartments analyzed, except in the Kenyon cell bodies (Figures 1C and 1D). AKAR2 can be detected in the α' and β' lobes with the *238Y* driver, but in vivo brain movements, and the fact that the α' and β' lobes are more weakly labeled than other lobes, prevented us from obtaining reliable FRET measurements in these lobes. As expected, FRET ratios return to baseline values after forskolin washout (Figures 1C and 1D). Importantly, this FRET increase was not accompanied by photobleaching of CFP or YFP (see Experimental Procedures). We were able to record PKA activity in vivo for at least 2 hr without observing any significant bleaching and/or decrease in FRET response amplitude to forskolin (data not shown). These results are consistent with changes corresponding to a FRET increase after PKA activation.

To verify that AC activation is responsible for the increase in FRET ratio, we used a forskolin analog that does not activate
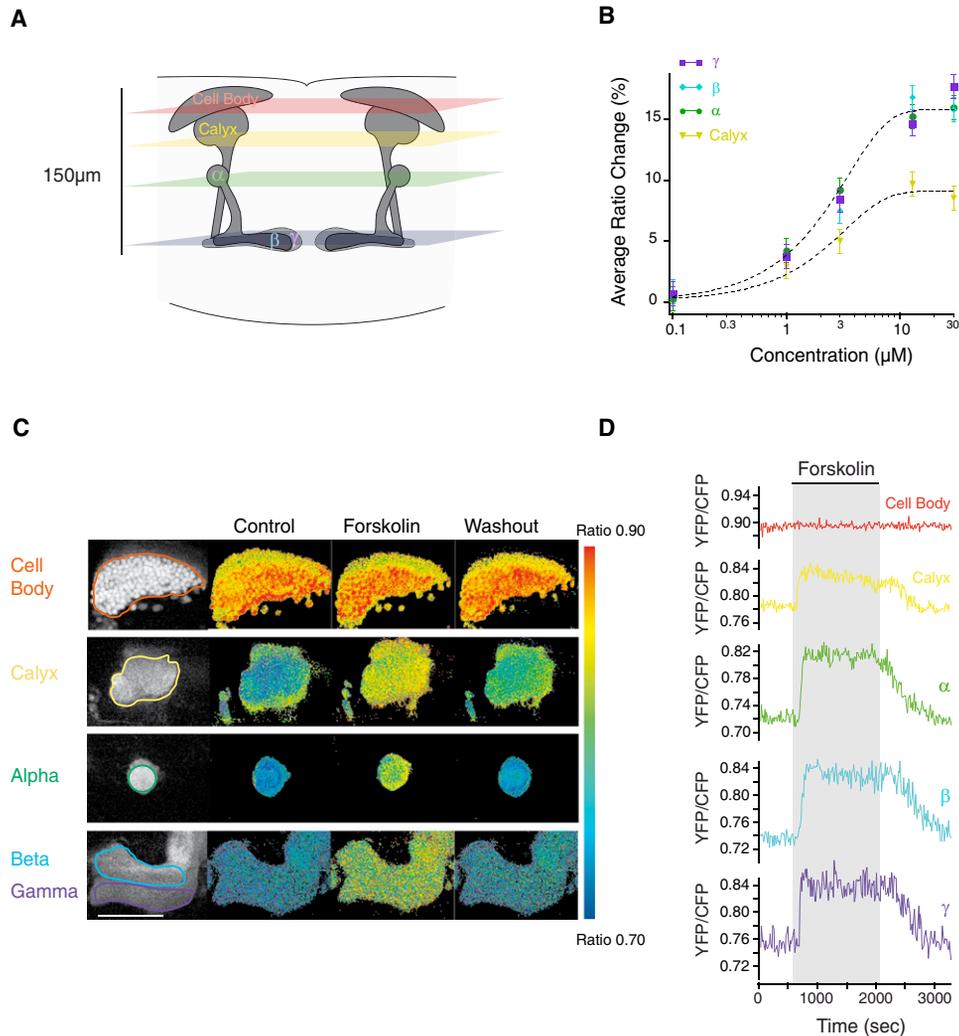
Figure 1. In Vivo Expression of AKAR2 in *Drosophila* MB Neurons

(A) Schematic representation of MB neurons in the adult brain and the z position of the FRET images acquired. The Kenyon cell bodies are clustered in the posterior and dorsal parts of the brain. MB neurons extend dendrites into the calyx and one axon through the peduncle toward the anterior and dorsal anterior parts of the brain. Except for γ axons, MB axons branch into vertically and horizontally oriented neuropil regions known as lobes. The α and α′ lobes project vertically and the β, β′, and γ lobes project horizontally.

(B) Dose-response curve of the AKAR2 sensor in MB in response to forskolin (n = 5).

(C) Images of basal AKAR2 fluorescence and pseudocolor responses of Kenyon cell bodies, calyx, and α, β, and γ lobes to bath application of forskolin. Grayscale images show the basal fluorescence of CFP at 820 nm. Pseudocolor images show the YFP/CFP ratio for each pixel coded using a look-up table. Images correspond to FRET under basal, forskolin-stimulated, and washout conditions. The scale bar represents 50 μm.

(D) Representative time course of YFP/CFP ratios in response to a bath application of forskolin (indicated by the gray shade on the graph) in the Kenyon cell bodies (red curve), calyx (yellow), and α (green), β (blue), and γ (purple) branches of the same living fly. The ratio was averaged over the regions outlined with the colored contour drawn in the grayscale image (B). See also Figure S1.

Data are expressed as mean ± SEM.

AC, 1,9-dideoxyforskolin (10 μM). This compound produces no FRET ratio change (Figures S2A and S2B). To further test the specificity of the AKAR2 probe for PKA, we used a cAMP analog that specifically blocks PKA, Rp-8-CPT-cAMPs (500 μM). In the presence of this PKA inhibitor, forskolin responses are reduced to approximately 20%–30% in axons and dendrites (Figures S2C and S2D). The fact that we did not observe a complete block of PKA activation by forskolin was expected because Rp-8-CPT-cAMPs is a competitive inhibitor of the cAMP-binding site, and

therefore its effects are weakened when endogenous levels of cAMP are high, such as after forskolin stimulation (Gjertsen et al., 1995). Together, these results confirm that forskolin-induced increases in FRET ratio are indeed a consequence of PKA activation.

MBs Display Compartment-Specific PKA Dynamics

Bath application of forskolin results in nonhomogeneous activation of PKA in the different subcellular compartments of the MB
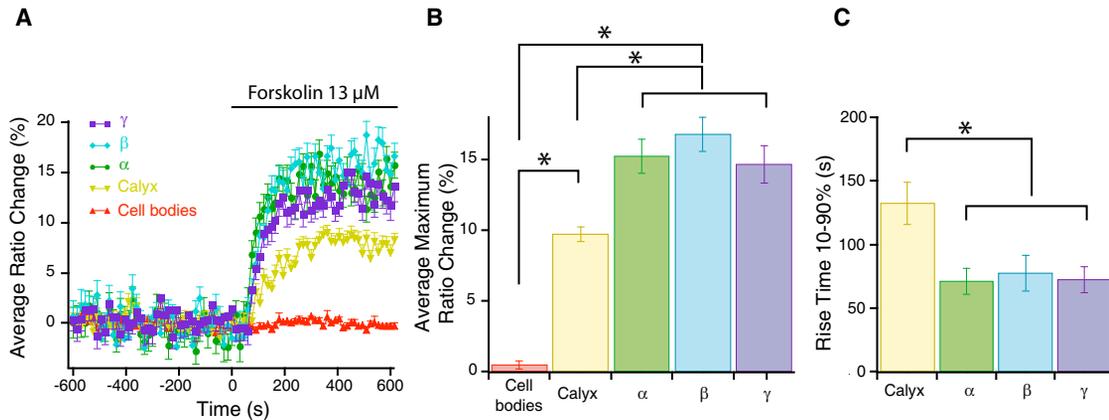
Figure 2. The Dynamic Range of PKA Activation in Response to Forskolin Application Is Larger in Axons than in Dendrites

(A) Time course of mean FRET ratios in Kenyon cell bodies (red triangles), calyx (yellow inverted triangles), and α (green circles), β (blue diamonds), and γ (purple squares) branches of MB neurons. Time 0 indicates the beginning of forskolin bath application. Each trace represents an average of 12 different flies.

(B) Mean FRET ratio changes in response to forskolin application for each MB neuron compartment. Calyces present a smaller response amplitude compared with axons ($p < 0.05$, $n = 12$).

(C) Comparison of the rise time (10%–90%) of forskolin-induced FRET ratios. Responses in the calyces are slower than in the lobes ($p < 0.05$, $n = 10$). See also Figure S2.

Data are expressed as mean ± SEM.

neurons (Figure 2A). Responses in dendrites (measured at the level of the calyces) are significantly smaller in amplitude than those observed in axons (measured at the level of α, β, and γ lobes) (Figure 2B). We did not detect significant differences in PKA activation by forskolin between the different lobes. Heterogeneity in forskolin response between axons and dendrites cannot be attributed to differences in basal FRET ratio (Vincent et al., 2008), and we found no correlation between this basal value and the maximal FRET ratio observed after forskolin application (Figures S2E and S2F).

The kinetics of PKA activation were estimated by measuring 10%–90% rise times. Rise times are significantly longer in dendrites than in axons (Figure 2C). This difference in kinetics cannot be attributed to forskolin diffusion, because the axons lie deeper in the brain than the calyces but respond faster (Figure 1A). The time course of forskolin-induced FRET is comparable in magnitude and onset to that reported for this sensor in mouse brain slices (Gervasi et al., 2007) and rat retinal ganglion cells (Dunn et al., 2006).

The Kenyon cell bodies display no significant FRET response to forskolin (Figure 2B; 0.48% ± 0.3% ratio change). The fluorescence intensity and the YFP/CFP ratio measured in the Kenyon cell bodies are both high, and are often above the maximum response observed in other subcellular compartments, as though the AKAR2 probe present in MB cell bodies were permanently phosphorylated (Figures 1B and 1C). However, the reason why the cell bodies fail to respond to forskolin application remains unknown and, for this reason, we decided to focus exclusively on the calyces and lobes in subsequent experiments.

In summary, we have shown that widespread brain AC stimulation leads to heterogeneous AKAR2 FRET responses in various MB compartments, suggesting that these subcellular domains are not equivalent in terms of PKA dynamics.

Altered PKA Dynamics in Learning and Memory Mutants Affecting the cAMP Pathway

Having established that the AKAR2 probe is suitable for monitoring PKA dynamics in the MBs, we studied in vivo how this pathway is affected in *rut* and *dnc* learning and memory mutants. We first generated a homozygous *UAS-AKAR2; 238Y-Gal4* strain, and verified that $rut^{2080}/Y;AKAR2/+;238Y/+$ males show a 2 hr memory defect comparable to that reported for rut^{2080} in previous studies (Figure 3A) (Han et al., 1992). Application of forskolin to the rut^{2080} mutant generates FRET ratio increases that are weaker than those observed in controls (Figure 3B). All neuronal compartments (α, β, γ, and calyces) show a similar reduction in the amplitude of the PKA response compared with controls. In terms of kinetics, we observed a general increase in the rise time of PKA signals in the rut^{2080} mutant (Figure 3C). Interestingly, heterozygous $rut^{2080}/+; AKAR2/+;238Y/+$ females show a normal 2 hr memory (Figure 3A) and a normal forskolin response in both amplitude and rise time (Figure S3).

It has been reported that cAMP concentrations are increased in the brain of the mutant dnc^1 (Byers et al., 1981), and we therefore investigated PKA dynamics in this mutant. We verified that $dnc^1/Y;AKAR2/+;238Y/+$ flies show a 2 hr memory deficit comparable to that reported for dnc^1 in other studies (Figure 3D) (Tully and Quinn, 1985). FRET responses in axons are significantly increased in dnc^1 mutant compared to wild-type control flies in response to bath application of forskolin. Interestingly, however, no difference in amplitude was recorded in the dendrites between dnc^1 mutant and wild-type flies (Figure 3E). No differences were also measured in the kinetics of the response to forskolin (Figure 3F). Heterozygous $dnc^1/+;AKAR2/+; 238Y/+$ females display normal 2 hr memory (Figure 3D) and normal forskolin responses with respect to both amplitude and rise time (Figure S3).
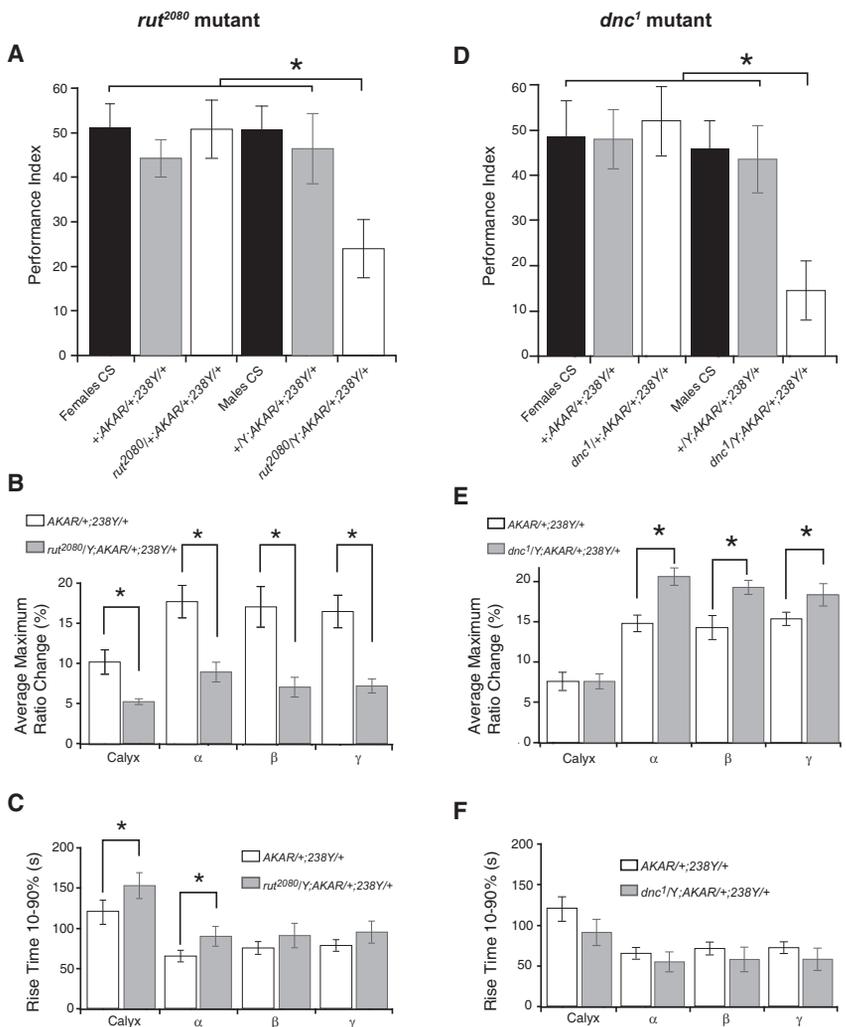
Figure 3. Learning and Memory Mutants Show Modifications in Forskolin-Induced PKA Activation

(A) Memory performance of flies 2 hr after a single training session. rut^{2080} mutant flies show a 2 hr memory deficit ($p < 0.05$, n = 12).

(B) Mean FRET ratio changes in response to forskolin in rut^{2080} and control flies. The FRET ratio change is lower in the rut^{2080} mutant compared with wild-type flies ($p < 0.05$, n = 12).

(C) In the rut^{2080} mutant, the FRET ratio rise time is significantly increased in the calyces and α lobes ($p < 0.05$, n = 10).

(D) Memory performance of flies 2 hr after a single training session. The dnc^1 mutant shows a 2 hr memory deficit ($p < 0.05$, n = 8).

(E) Mean FRET ratio changes in response to forskolin in dnc^1 and control flies. FRET ratio changes increase in the dnc^1 mutant exclusively in the MB lobes ($p < 0.05$, n = 8).

(F) Mean FRET ratio kinetics in response to forskolin in dnc^1 and control flies. No significant differences were found between the two genotypes (n = 8). See also Figure S3.

Data are expressed as mean ± SEM.

activity of ACs and PDEs present in the dendrites and axons of wild-type flies.

In dnc^1 mutants, IBMX application has no effect on PKA activation, confirming that Dnc PDE is indeed inhibited by IBMX in control flies (Figures 4A and 4B). Addition of forskolin in the presence of IBMX produced an identical increase in FRET ratio in control and dnc^1 flies (Figures 4A and 4B), showing that a specific lack of Dnc function or a general pharmacological inhibition of PDEs leads to the same maximal forskolin response. Dnc is therefore the only (or at least the main) PDE active in the adult α/β and γ neurons.

In the rut^{2080} mutant, application of IBMX alone produces a level of PKA activation similar to that observed in control flies (Figures 4C and 4D). Moreover, no differences in the kinetics of the response to IBMX were observed between wild-type and rut^{2080} flies (data not shown). These results indicate that Rut is not the AC involved in the PKA response observed in response to IBMX in the absence of forskolin stimulation. Our experiments therefore reveal the existence of a basal pool of cAMP produced by a Rut-independent AC and regulated by Dnc PDE in MBs.

In summary, learning and memory mutants carrying defects in key enzymes of the cAMP pathway present drastic alterations of PKA dynamics in the MBs. For both mutants, modification of the regulation of PKA activity is revealed by forskolin application. In the rut^{2080} mutant, the AKAR2 response is weaker than in the control, but not abolished. Because rut^{2080} is reported to be a null mutation (Levin et al., 1992), this residual PKA activity is probably due to the existence of another AC expressed in the MBs. In dnc^1 flies, we observed an increase of forskolin-induced activation of PKA in MB axons compared to controls, but not in dendrites.

Rut AC Is Only Active after MB Stimulation Whereas a Rut-Independent AC Shows Basal Activity

In the dnc^1 mutant, the loss of PDE activity is constitutive during development and in the adult. We wished to look at the effect of a transient inhibition of PDEs using a bath application of IBMX, an inhibitor of most PDEs at 200 μM (Beavo et al., 1970). In $AKAR2/+;238Y/+$ flies, IBMX application alone produces a homogeneous increase in FRET ratio in MB neuronal compartments (Figures 4A and 4B). This PKA activation reflects a tonic

Uniform Dopamine Stimulation Activates PKA Specifically in the MB α Lobes

Formation of aversive and appetitive memories requires dopamine and octopamine, respectively, to sustain the US pathway. To investigate the effect of these neuromodulators on PKA activity, we bath applied either dopamine or octopamine. Surprisingly, dopamine produces a concentration-dependent increase in FRET ratio specifically in the α lobes, and no

A

B

C

D
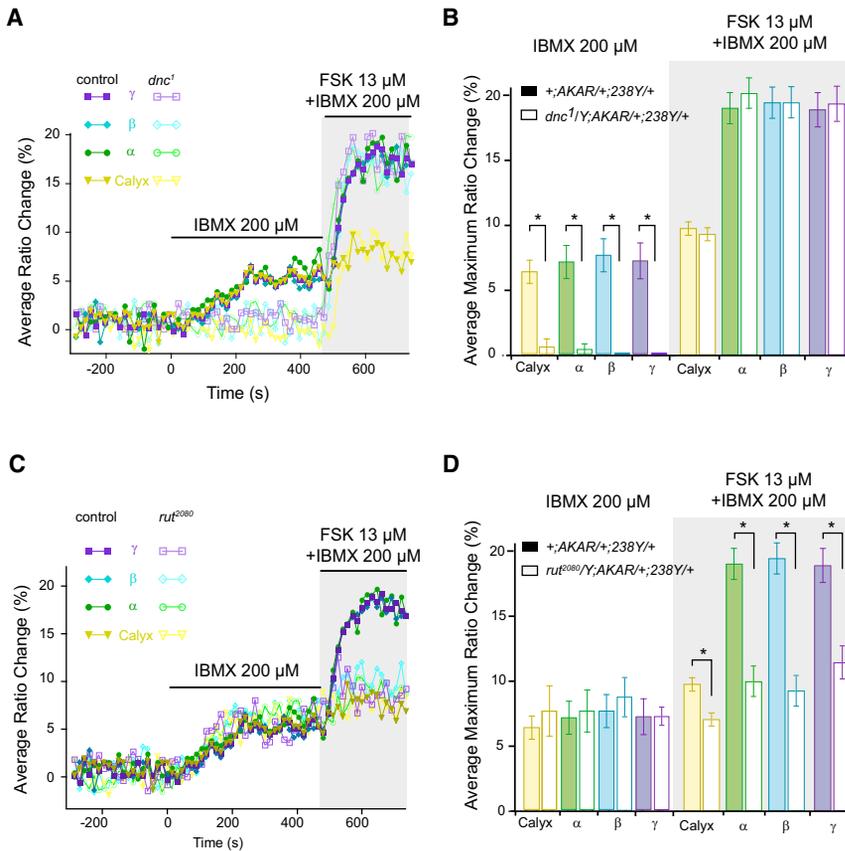
Figure 4. Rut-Independent Basal AC Activity Is Regulated by Dnc PDE in the MBs

(A) Representative FRET ratio time course in response to 200 μM IBMX observed in *dnc¹* and control flies. Responses of a *dnc¹* mutant fly in the calyx (yellow open triangles) and α (green open circles), β (blue open diamonds), and γ (purple open squares) branches compared with wild-type calyx (yellow triangles) and α (green-circles), β (blue diamonds), and γ (purple squares) branches. IBMX has no effect on *dnc¹* flies. Flies were also stimulated by forskolin to verify that FRET ratio changes are similar in *dnc¹* and control flies in the presence of IBMX.

(B) Mean FRET ratio changes in response to IBMX in *dnc¹* and control flies (p < 0.05, n = 5). The FRET response to forskolin was similar in the two groups (n = 5), indicating that Dnc PDE is the main enzyme regulating cAMP concentration in the MBs.

(C) Representative FRET ratio time courses in response to 200 μM IBMX in a *rut²⁰⁸⁰* and a control fly. Responses of the *rut²⁰⁸⁰* mutant in the calyx (yellow open triangles) and α (green open circles), β (blue open diamonds), and γ (purple open squares) branches compared with those of wild-type calyx (yellow triangles) and α (green circles), β (blue diamonds), and γ (purple squares) branches. IBMX produced the same FRET ratio increase in *rut²⁰⁸⁰* flies, indicating that Rut AC is not responsible for basal cAMP synthesis in the MBs.

(D) Mean FRET ratio changes in response to IBMX show no significant differences between *rut²⁰⁸⁰* and control flies (n = 5). The FRET response to forskolin is decreased in *rut²⁰⁸⁰* flies (p < 0.05, n = 5). *+;AKAR2/+;238Y/+* control flies are identical in (B) and (D).

Data are expressed as mean ± SEM.

significant increase was observed in the β and γ lobes or in the calyces (Figures 5A and 5C). In contrast, octopamine evokes a concentration-dependent increase of FRET ratio in all MB compartments (Figures 5B and 5D). After dopamine or octopamine responses, we applied forskolin to test the maximal response of the AKAR2 probe. No significant differences were observed in forskolin response between dopamine-stimulated flies and octopamine-stimulated flies (Figures 5A2 and 5B2). Both dopamine and octopamine FRET responses were blocked by the specific PKA antagonist Rp-8-CPT-cAMPs (Figure S4A).

The striking difference between dopaminergic and octopaminergic PKA activation patterns likely reflects a fundamental property of the *Drosophila* brain, rather than the experimental conditions used, because (1) octopamine and dopamine are structurally similar amines, (2) a recent study showed that a 1 s pulse of dopamine applied locally to the *Drosophila* brain can be detected in less than 5 s at a depth of about 10 μm (Makos et al., 2009), and so bath application of the *Drosophila* brain for several minutes should allow dopamine to reach the medial lobes, and (3) the time course of dopamine reuptake is about 50 s, which is rather slow (Makos et al., 2009). The specific localization of dopamine-induced PKA activation is therefore most likely not due to a problem of diffusion or dopamine reuptake in the living *Drosophila* brain.

Appetitive learning depends on motivational state, as flies must be hungry to form appetitive memory (Krashes and Waddell, 2008; Colomb et al., 2009). This motivational control of appetitive memory formation is sustained by a neuronal circuit that directly regulates MB neurons (Krashes et al., 2009). We tested the hypothesis that motivational state can modify octopaminergic signals in MB neurons by bath application of octopamine on 21 hr food-deprived flies. FRET ratio responses were similar in control and food-deprived flies (Figure 5D), showing that the motivational state of the fly did not affect octopaminergic signaling.

To test whether the α lobe-specific activation of PKA by dopamine reflects an intrinsic property of the MBs, we pharmacologically abolished brain activity using TTX (1 μM), a neurotoxin that blocks action potentials through the blockade of voltage-sensitive sodium channels (Narahashi et al., 1964). Forskolin application leads to the same response amplitude with or without TTX (Figure S4B). Moreover, bath application of dopamine in the presence of TTX still results in α lobe-specific PKA activation (Figure 5C). The homogeneous PKA activation observed in MBs after octopamine application was also similar in control flies and TTX-treated flies (Figure 5D). Thus, dopamine- and octopamine-induced PKA activity is not due to a network effect acting on the MBs but rather reflects an autonomous property of the MB neurons themselves.

A1

Ratio=.75   Control   Dopamine

Ratio=.70

A2

A3

B1

Ratio=.80   Control   Octopamine

Ratio=.72

B2

B3

C

D

E

(E) Mean FRET ratio changes in response to dopamine and octopamine in *rut*[2080] and control flies. Dopamine-induced FRET ratio responses were Rut dependent (n = 9). Octopamine-induced FRET ratio responses were Rut dependent (n = 7). See also Figure S4.
Data are expressed as mean ± SEM.
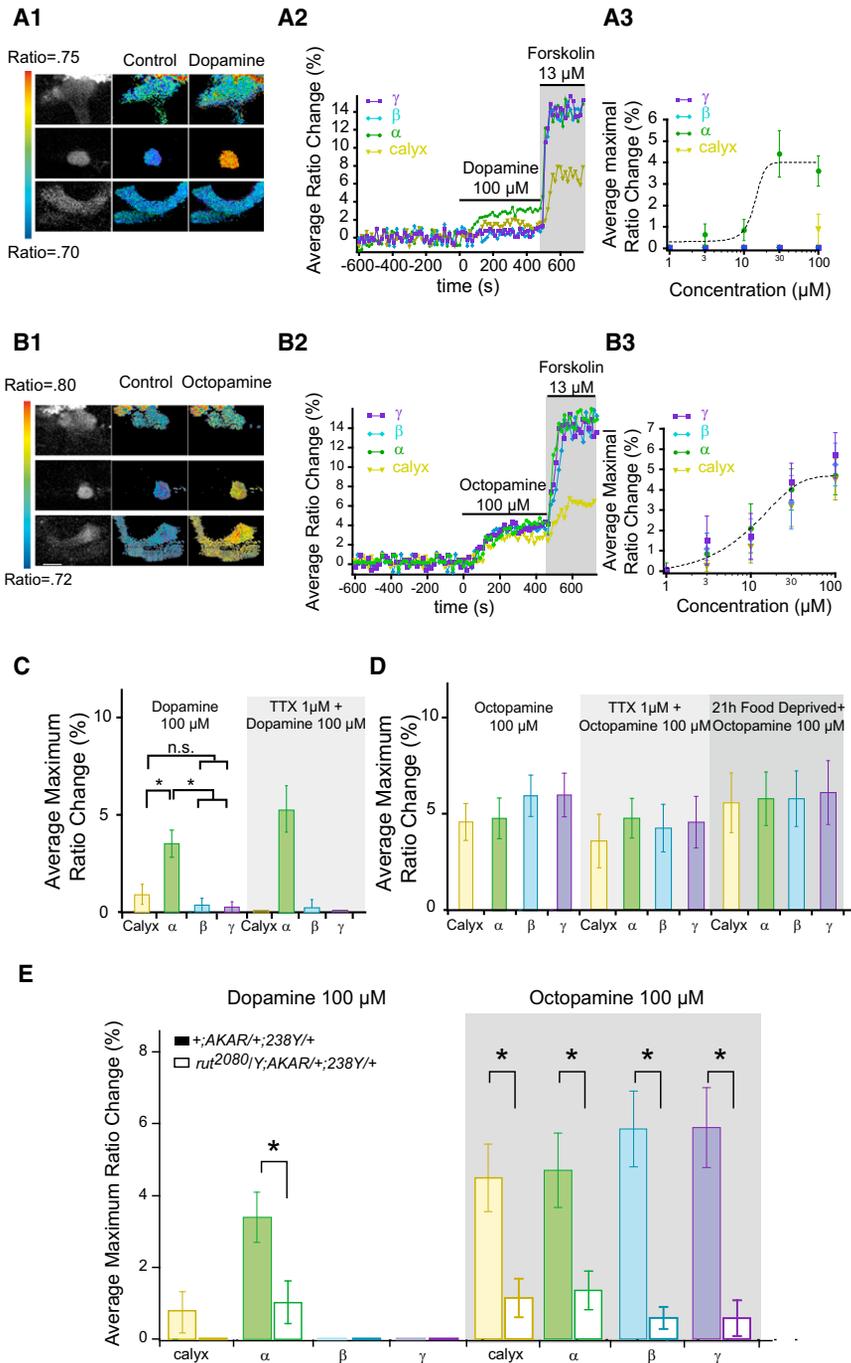
Figure 5. Dopamine Application Specifically Activates PKA in the α Lobe in a Rut-Dependent Manner whereas Octopamine Induces a Rut-Dependent Activation of PKA in All MB Lobes and Calyx

(A1) Images of basal AKAR2 fluorescence and pseudocolor responses of the calyx and α, β, and γ lobes to bath application of 100 μM dopamine. Grayscale images show the basal fluorescence of CFP at 820 nm, and pseudocolor images correspond to basal and dopamine-stimulated FRET ratios.

(A2) Representative time course of FRET ratios in response to bath application of dopamine (indicated by the black bar) and forskolin (indicated in gray) in the calyx (yellow triangles) and α (green circles), β (blue diamonds), and γ (purple squares) branches, recorded in the same fly.

(A3) Dose-response curve for MB responses to bath-applied dopamine (n = 6). Please note that the symbols for the β lobes and calyx are hidden by the symbols for the γ lobes.

(B1) Images of basal AKAR2 fluorescence and pseudocolor responses of the calyx and α, β, and γ lobes to bath application of 100 μM octopamine. Grayscale images show the basal fluorescence of CFP at 820 nm, and pseudocolor images correspond to basal and octopamine-stimulated FRET ratios.

(B2) Representative time course of FRET ratios in response to octopamine bath application (indicated by the black bar on the graph) and forskolin (indicated by the gray shade on the graph) in the calyx (yellow triangles) and α (green circles), β (blue diamonds), and γ (purple squares) branches recorded in the same fly.

(B3) Dose-response curve for MB responses to bath-applied octopamine (n = 6). Please note that the symbols for the α lobes, β lobes, and calyx are hidden by the symbols for the γ lobes.

(C) Mean FRET ratio changes in response to dopamine (p < 0.05, n = 9). A 10 min bath application of TTX (1 μM) was used to block action potentials in the entire *Drosophila* brain. Dopamine was then applied. The same pattern of dopamine-induced PKA activation is seen in the presence or absence of TTX (n = 4).

(D) Mean FRET ratio changes in response to octopamine (n = 7). Pretreatment with 1 μM TTX has no effect on PKA activation (n = 4). For food-deprivation experiments, flies were kept in plastic bottles with cotton wool pads imbibed with 6.5 ml of mineral water for 21 hr. Octopamine bath application produces a similar level of PKA activation to that in control flies (n = 6).

We then tested the involvement of the Rut AC in responses to dopamine and octopamine. In the *rut*[2080] mutant, the responses to both dopamine and octopamine are greatly reduced and close to experimental noise (Figure 5E). The effects of dopamine and octopamine on PKA activation in MB neurons are therefore Rut dependent.

Rut AC Synergistically Activates PKA by Associating Two Subthreshold Stimuli

Because Rut AC functions as a putative molecular coincidence detector, we tested the effect on PKA activation of pairing of acetylcholine (which represents the conditioned stimulus pathway during olfactory associative conditioning) with dopamine
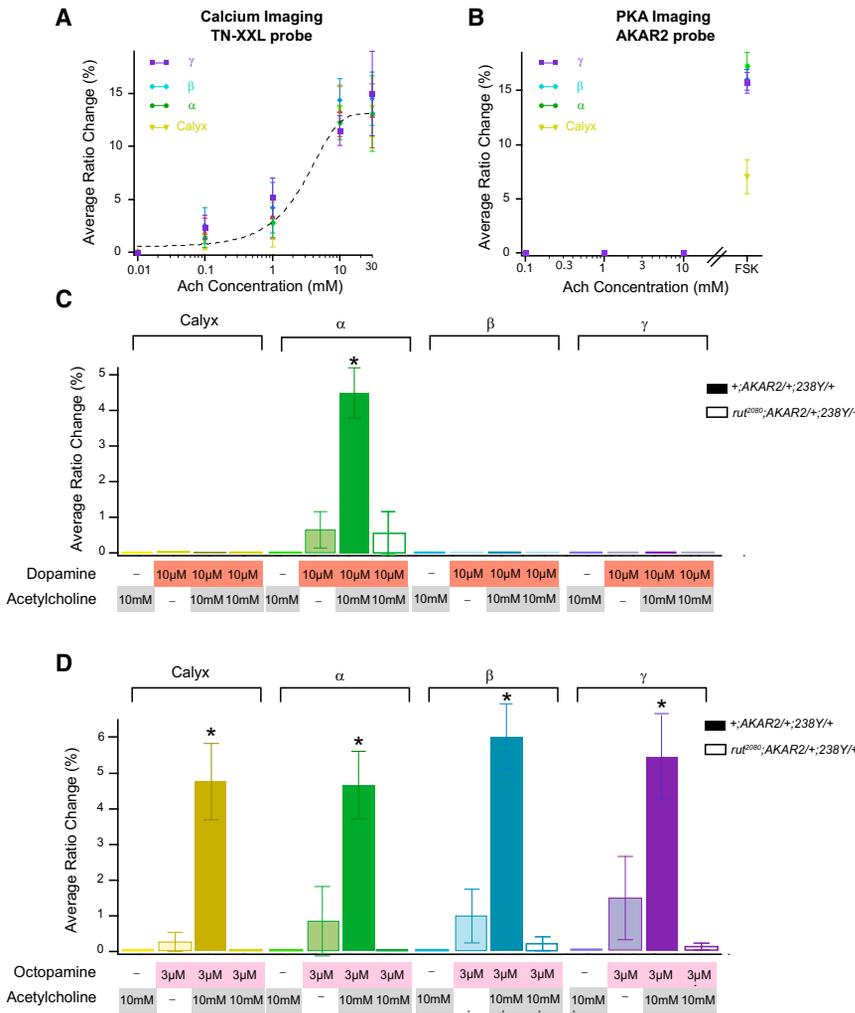
Figure 6. Pairing of an Acetylcholine-Mediated Intracellular Calcium Increase with Dopamine or Octopamine Induces a Rut-Dependent Synergistic Activation of PKA in MB Neurons

(A) Dose-response of MB neurons expressing TN-XXL probes in the MBs in response to acetylcholine bath application (n = 6).

(B) Dose-response of MB neurons expressing the AKAR2 probe in the MBs in response to acetylcholine and forskolin bath application (n = 6).

(C) Mean FRET ratio changes in response to 10 mM acetylcholine, 10 μM dopamine, or paired application of acetylcholine and dopamine in control and rut^{2080} flies (n = 6). Pairing produces an activation of PKA only in the α lobes of the MBs (p < 0.05). This potentiation of dopaminergic signaling is ablated in the rut^{2080} mutant.

(D) Mean FRET ratio changes in response to 10 mM acetylcholine, 3 μM octopamine, or paired application of acetylcholine and octopamine in control and rut^{2080} flies (n = 6). Pairing produces an activation of PKA in all lobes of the MBs (p < 0.05). This potentiation of octopaminergic signaling is ablated in the rut^{2080} mutant. See also Figure S5.

Data are expressed as mean ± SEM.

or octopamine (which represent the aversive and appetitive unconditioned stimuli). We first verified that acetylcholine increases intracellular calcium in our setup. We used the genetically encoded calcium indicator TN-XXL, which has previously been used for in vivo multiphoton imaging (Mank et al., 2008). We observed that acetylcholine increases intracellular calcium in a concentration-dependent manner in all MB compartments, including the cell bodies (Figure 6A). Application of 30 mM KCl after 10 mM acetylcholine stimulation further increases the FRET ratio, showing that the plateau observed with high concentrations of acetylcholine does not represent TN-XXL saturation (data not shown). We next turned to AKAR2 imaging and showed that 10 mM acetylcholine does not activate PKA in the MBs (Figure 6B). After acetylcholine application, we verified that flies responded normally to forskolin (Figure 6B). Finally, we paired acetylcholine at a concentration that produces a maximal calcium response (10 mM) with dopamine or octopamine at concentrations that produce partial PKA activation (10 μM and 3 μM, respectively). Pairing with acetylcholine leads to a strong increase in PKA activation compared with stimulation with dopamine or octopamine alone (Figures 6C and 6D), even though acetylcholine alone does not activate PKA. This synergistic

effect is abolished in the rut^{2080} mutant (Figures 6C and 6D), demonstrating the involvement of Rut AC in the process of stimulus integration. The spatial restriction of PKA activity in MB α lobes by dopamine was notably conserved in the presence of acetylcholine. We also paired acetylcholine with dopamine and octopamine at concentrations that alone produce maximal PKA activation (100 μM). These pairings changed neither the amplitude nor the spatial activation pattern of PKA (Figure S5).

These data demonstrate that increased intracellular calcium combined with application of dopamine or octopamine at subthreshold concentrations generates a synergistic Rut-dependent activation of PKA in MBs. This coincidence detector behavior produces a left shift of the dose-response curve, with no changes in the spatial dynamics of PKA activation.

Dunce Activity Compartmentalizes Dopamine-Induced PKA Activation to the MB α Lobes

As the activity of PDEs has been proposed to regulate PKA activation by neuromodulators in various cell types (Conti and Beavo, 2007), we examined the regulation of dopamine and octopamine signaling by Dnc PDE. FRET responses to octopamine are identical in dnc^1 mutants compared with those observed in normal flies (Figure 7B). In contrast, the α lobe specificity of PKA activation that follows dopamine application is abolished in the dnc^1 mutant, as dopamine produces an increase in the FRET emission ratio of the α, β, and γ lobes and calyces (Figure 7A). Dnc PDE therefore specifically regulates dopaminergic
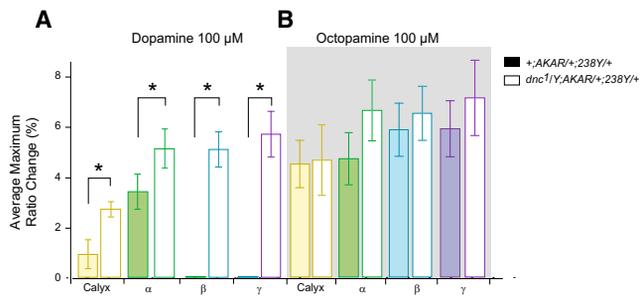
Figure 7. Dnc PDE Is Required for the α Lobe Specificity of Dopamine-Induced PKA Activation

Mean FRET ratio changes in response to dopamine (A) and octopamine (B) in *dnc¹* and control flies. Dopamine induced a FRET ratio change in all MB compartments in *dnc¹* mutant flies (p < 0.05, n = 9). No differences were observed in octopamine-induced FRET ratio responses between *dnc¹* and control flies (n = 7). *+;AKAR2/+;238Y/+* control flies are identical in (A) and (B). Data are expressed as mean ± SEM.

signaling in MB neurons by restricting dopamine-induced PKA activation to the α lobe of the MBs.

DISCUSSION

Subcellular PKA Dynamics in the MBs

The recent development of genetically encoded probes for PKA activity has provided the means to measure PKA signaling with unprecedented sensitivity and temporal resolution. These probes have been used to observe PKA activity in HEK cells (Zhang et al., 2005), cardiomyocytes (Saucerman et al., 2006), the explanted neonatal retina (Dunn et al., 2006), and brain slices (Gervasi et al., 2007). Here we show that two-photon microscopy with the AKAR2 probe provides an excellent platform with which to observe PKA dynamics within identified neurons of a living *Drosophila* adult brain.

Our experiments show that PKA has a larger dynamic range of activity in MB axons than in dendrites, whereas cell bodies present no FRET change in response to forskolin. The fact that a spatial gradient in PKA response is observed in response to a uniformly applied AC activator points to the existence of functional subdivisions within the MBs for this signaling pathway. This functional compartmentalization of the *Drosophila* MBs could result from several factors. For example, the activity gradient may be caused by a heterogeneous distribution of proteins that compose the signaling pathway, in particular AC. An in silico study has shown that AC appears to be a stoichiometrically limiting step in cAMP synthesis, and that the cAMP concentration measured should be linearly proportional to AC activation (Saucerman et al., 2003). In MB neurons, Rut protein is preferentially expressed in the α, β, and γ branches (Han et al., 1992). These MB axons should therefore have faster kinetics and reach a higher level of PKA activity because they contain higher levels of AC.

In addition, the physical properties of the different neuronal subcellular domains may have an impact on cAMP/PKA signal integration (Neves et al., 2008). For example, surface area to volume ratios favor the accumulation of cAMP in neurites, as demonstrated in *Aplysia* sensory neurons (Bacskai et al., 1993)

and the lobster stomatogastric ganglion (Hempel et al., 1996). This spatial disposition would facilitate fast and local activation of PKA in axons, whereas filling the cell body with cAMP would be less efficient. The attenuation of the PKA signal as it approaches the cell body could serve as a filtering or integrating mechanism, for example to control the transition between short-term and long-term memory. Thus, only long-term memory formation would involve PKA-dependent activation of transcription factors that regulate de novo protein expression (Yin et al., 1994).

Blocking PDEs in the absence of artificial AC activation leads to increased PKA activity, suggesting that a tonically active AC is present in MBs. However, in the context of basal levels of PDE activity, PKA inhibition by Rp-8-CPT-cAMPs did not lead to a decrease in FRET ratio, indicating that under normal conditions, tonically synthesized cAMP does not reach the threshold for PKA activation and/or AKAR2 phosphorylation. This tonically active AC does not correspond to Rut, because PKA activity after PDE blockade is similar in the *rut* mutant and the wild-type control. In fact, a Rut-independent AC has previously been identified in the *Drosophila* brain (Livingstone et al., 1984; Dudai, 1985). Constitutive AC activity has also been recorded in neurons of the *Drosophila* circadian clock (Shafer et al., 2008), and seems to be a common property of neurons in many species (Gervasi et al., 2007; Vincent et al., 2008). In the *rut* mutant, forskolin still results in activation of PKA, suggesting that the tonically active AC can be overstimulated. However, unlike Rut, the Rut-independent AC is not activated by dopamine and octopamine. This tonically active system may be regulated by different, nonassociative signaling pathways. Because we performed in vivo recordings, we cannot exclude the possibility that this "tonic" cAMP production is a result of sensory and neuromodulatory inputs that activate the Rut-independent AC.

A recent cAMP imaging study of the *Drosophila* MBs reported dopamine- and octopamine-induced cAMP increases independent of Rut AC (Tomchik and Davis, 2009). The authors observed dose-response curves of cAMP/PKA pathway stimulation shifted to the right in comparison with our study, which is likely due to the fact that the epac1-camps probe has an EC_{50} for cAMP of 2.4 μM (Nikolaev et al., 2004), whereas the PKA regulatory subunit has an EC_{50} of around 100–500 nM (Taylor et al., 1990). A modeling analysis has estimated that the free cAMP in the soma is under μM concentration during physiological stimulation (Neves et al., 2008). We therefore propose that Rut-independent dopaminergic and octopaminergic activation occurs only at high neuromodulator concentrations.

Alteration of Spatiotemporal PKA Dynamics in Learning and Memory Mutants

The *rut* mutant displays a learning and/or short-term memory defect (Livingstone et al., 1984) and specifically lacks Ca^{2+}/calmodulin-stimulated AC activity (Livingstone et al., 1984; Livingstone, 1985). It has been suggested that this enzyme represents a molecular integration site during associative learning (Dudai, 1985). Indeed, it has been shown that Rut AC can be activated by Ca^{2+}/calmodulin as well as through G protein stimulation (Levin et al., 1992). These two pathways could represent at the molecular level the olfactory stimulus
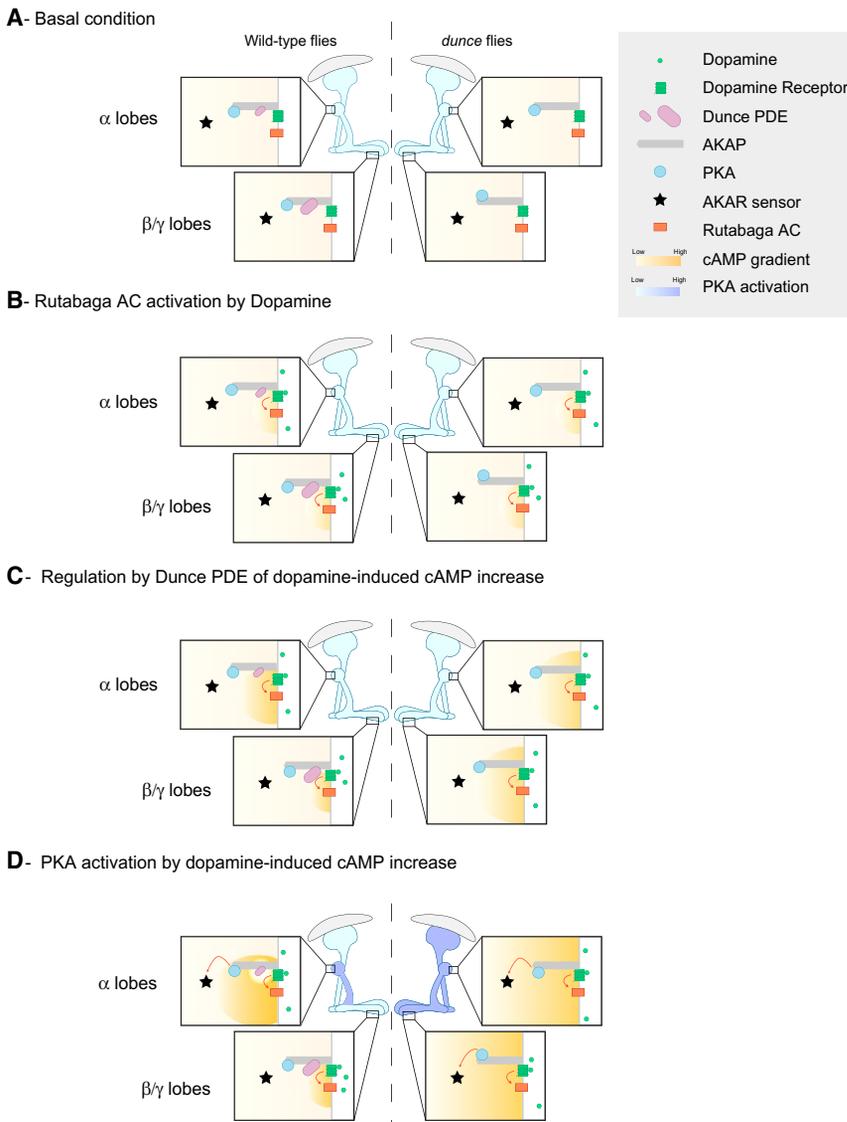
Figure 8. Molecular Model for Dopamine-Induced PKA Activation in the MB α Lobes

A schematic diagram showing a possible model for the restriction of dopamine-induced PKA activity to the α lobes.

(A) In the basal state, PKA does not appear to be activated because application of Rp-8-CPT-cAMPs does not change the AKAR2 FRET ratio.

(B) Bath application of dopamine activates a D1-type dopamine receptor located in all MB lobes. This receptor is a Gs protein-coupled receptor that activates Rut AC. This activation initiates cAMP production.

(C) In the medial lobes, PKA, PDE, AC, and the dopamine receptor are kept in close proximity due to their association with an AKAP protein. Dnc PDE efficiently hydrolyzes the cAMP produced by Rut AC, and the cAMP concentration around PKA does not reach the threshold for its activation. In the vertical lobes, PKA, PDE, AC, and the dopamine receptor are also associated with an AKAP but, for an unknown reason, Dnc PDE is less efficient at hydrolyzing cAMP. As a consequence of this reduced degradation, cAMP molecules start diffusing in the cytosol.

(D) In vertical lobes, the cAMP reaches the PKA pool close to Rut AC. PKA is activated and phosphorylates its targets such as the AKAR2 probe. In the *dnc* mutant, dopamine activates Rut AC associated with its receptor. In the absence of the major source of PDE activity in the MBs, cAMP degradation is reduced. The cAMP produced by Rut AC in response to dopamine can therefore diffuse more widely and activate PKA in all MB compartments.

and the US (electric shock or sugar) that converge onto the MBs. The olfactory information is carried by projection neurons that release acetylcholine at the MB calyces. Dopamine has been shown to correspond to the aversive US, and octopamine to the appetitive US, and both increase cAMP concentration in vitro (Han et al., 1996, 1998; Schroll et al., 2006; Thum et al., 2007; Claridge-Chang et al., 2009). MB-specific expression of Rut AC in an otherwise *rut* mutant brain rescues performance of aversive and appetitive olfactory memories (Zars et al., 2000; McGuire et al., 2003; Schwaerzel et al., 2003; Blum et al., 2009). Our data support the view that Rut AC acts as a coincidence detector that associates the US and the CS pathway in MB neurons. Consistent with this, we show that low concentrations of dopamine or octopamine activate PKA only if these neuromodulators are paired with an intracellular calcium increase produced by acetylcholine. This potentiation of dopaminergic and octopaminergic signaling is ablated in *rut* mutants. A parallel study, performed on isolated brains, similarly reported

a Rut-dependent synergistic increase in cAMP when acetylcholine was paired with dopamine. However, no positive synergistic effect was observed when acetylcholine was paired with octopamine (Tomchik and Davis, 2009), possibly because the authors use a saturating concentration of octopamine in their pairing experiment. At this concentration, we too did not observe potentiation of octopamine signaling, probably because PKA activity is saturated. Thus, the synergistic effect of pairing with acetylcholine is observed only at lower octopamine concentrations. We show that PKA responses to dopamine and octopamine are strongly diminished in rut^{2080} mutant. Thus, in *rut* flies, hypoactivity of the cAMP/PKA pathway in response to neuromodulator release should in turn disrupt the transduction of sensory information, and ultimately will produce a loss of coincidence detection that leads to defects in structural and functional plasticity (Zhong and Wu, 1991, 2004).

In various organisms, PDEs are one of the major contributors to PKA-mediated phosphorylation gradients (Conti and Beavo, 2007). In cardiomyocytes, the AKAR2 probe has been used to show that PDEs produce phosphorylation gradients by providing a sink for cAMP spatially separated from its source. PDE inhibition reduces the phosphorylation gradient by globally increasing

the concentration of cAMP (Saucerman et al., 2006). *Drosophila dnc* flies are defective in aversive learning and memory and in appetitive memory (Dudai et al., 1976; Tempel et al., 1983). A lack of Dnc PDE is associated with generally elevated levels of cAMP in the *Drosophila* brain (Byers et al., 1981; Davis and Kiger, 1981). Our analysis goes one step further, as we show that Dnc plays a key role in the regulation and the localization of cAMP/PKA dynamics in the MBs in that (1) forskolin-induced PKA activation in *dnc¹* is higher than that in wild-type flies, (2) the effect of the *dnc¹* mutation on forskolin-induced PKA activation is only observed in the axons of the MBs, and (3) α branch-specific PKA activation by dopamine is abolished in the *dnc¹* mutant (discussed in the next section). The behavioral defect of *dnc* mutant flies is therefore likely to be not only due to an increase in PKA activity but also, more importantly, to a loss of spatial and temporal specificity in the activation of the cAMP/PKA pathway. Because PKA activation reached similar levels in *dnc¹* flies and in wild-type flies treated with the broadly specific PDE inhibitor IBMX, we conclude that Dnc is the main PDE that regulates cAMP signals in MBs.

Aversive and Appetitive Neuromodulators Activate PKA in a Spatially Distinct Manner

We have shown that bath application of dopamine leads to activation of PKA specifically in the vertical lobes of the MBs, whereas no PKA activity was detected in the horizontal lobes. This result was unexpected, because dopamine receptors dDA1 and DAMB, which are positively coupled to AC, are equally distributed in all MB lobes, as are the PKA catalytic subunit DCO and Rut AC (Han et al., 1992, 1996; Kim et al., 2003). Thus, one would expect that the uniform application of dopamine would activate both the horizontal and vertical branches of MBs. Our data indicate that it is Dnc PDE that restricts dopamine-induced PKA activation to the α lobes, presumably by preferentially degrading cAMP in the medial β and γ lobes. This compartmentalization of functional dopaminergic signals in the α lobe is particularly interesting, especially in light of behavioral studies which have revealed an intriguing branch specificity in the formation of the aversive olfactory memory trace. For example: (1) *ala* mutants that lack α/α′ vertical lobes show no aversive long-term memory (Pascual and Preat, 2001; Isabel et al., 2004), (2) increases in calcium influx in response to presentation of a conditioned odor occur specifically in the α branch of the α/β MB neurons (Yu et al., 2006), and (3) a delayed olfactory short-term memory trace has been established in the dorsal paired medial neuron branch that innervates the vertical MB lobes, and not in the branch that innervates the horizontal MB lobes (Yu et al., 2005).

Dopaminergic neurons strongly innervate the vertical branch of the MBs, the γ spur, the medial lobes, and the calyx (Riemensperger et al., 2005; Mao and Davis, 2009). Recent studies suggest that the dopaminergic network is functionally subdivided. Calcium imaging studies have shown that the PPL1 dopaminergic neurons which project to the vertical lobes respond specifically to both odor and electric shock (Mao and Davis, 2009). Moreover, two elegant studies have shown that (1) genetically targeted optical activation of dopaminergic neurons projecting to the vertical lobes and the heel is sufficient for writing aversive olfactory memories (Claridge-Chang et al.,

2009), and (2) dopaminergic MB-MP neurons that project to medial lobes and the peduncle (Tanaka et al., 2008) control *Drosophila* motivational state (Krashes et al., 2009). Considered together, these studies show that dopaminergic inputs are required not only on the vertical lobes but also on other regions of the MB. In addition, expression of Rut in the γ lobes was shown to be necessary (Akalal et al., 2006) and sufficient (Zars et al., 2000; Blum et al., 2009) for normal short-term memory. To reconcile these data with the fact that we did not observe PKA activation in medial lobes after uniform dopamine stimulation, we propose the existence of microdomains of PKA activity that remain undetected by the AKAR2 probe. However, our work shows that, in addition to local modulations by discrete ensembles of dopaminergic neurons, MB neurons have an intrinsic propensity for spatially restricted PKA activation after dopamine stimulation, independent of the neuronal network.

We have shown that a uniform application of octopamine, a neuromodulator involved in appetitive memory, results in strong PKA activation in the α, β, and γ lobes and calyces. This effect is consistent with the location of the octopamine receptor OAMB in the calyces and MB lobes (Han et al., 1998), and with our observation that PDEs do not regulate octopaminergic signal transduction spatially, as was the case for dopamine. Octopaminergic neurons innervate the entire calyx and the spur of the γ lobe, but not the β and vertical lobes (Sinakevitch and Strausfeld, 2006; Busch et al., 2009). In addition, synaptic terminals of projection neurons receive octopaminergic projections, in particular those contacting the MB calyces (Sinakevitch and Strausfeld, 2006). Projection neurons, like MB neurons, display an appetitive memory trace, as Rut AC is sufficient in either set of neurons for normal appetitive learning (Schwaerzel et al., 2003; Thum et al., 2007). The calyces, which receive input from both projection neurons (carrying olfactory information) and octopaminergic neurons (carrying US information), could play an important role in the formation of appetitive memory traces.

The differences between dopamine- and octopamine-induced activation of PKA in the MBs have strong implications for our understanding of the molecular events underlying aversive and appetitive memory formation in *Drosophila*. Interestingly, in the appetitive paradigm, *dnc* flies exhibit normal learning and initial memory (Tempel et al., 1983), suggesting that Dnc PDE does not regulate PKA signaling in response to sugar presentation and its neurophysiological correlate, octopamine release. Our observation that Dnc PDE does not regulate PKA-mediated octopaminergic signaling in the MBs strengthens this view. In contrast, Dnc plays a major role in aversive olfactory learning and memory (Tully and Quinn, 1985) and, in support of this, we now show that Dnc PDE regulates PKA signaling in the MBs in response to dopamine treatment. Which mechanisms ensure that the same pathway is differentially regulated during aversive and appetitive learning so that the α lobe may specifically encode an aversive trace? An elegant study showed that AKAP-bound PKA plays a role in aversive but not appetitive memory (Schwaerzel et al., 2007). Scaffold proteins termed A kinase-anchoring proteins (AKAPs) are involved in the spatial and temporal regulation of signaling pathways (Wong and Scott, 2004). Interactions between PKA and PDE are mediated by AKAPs, which anchor

these macromolecular complexes in defined subcellular domains (Beavo and Brunton, 2002). Such interactions generate microdomains of PKA signaling in which local PDE regulates PKA activity and is itself regulated by phosphorylation to create a feedback loop (Dodge-Kafka et al., 2005). Based on the experiments of Schwaerzel et al. and our imaging study, we propose that aversive memory processing is specifically linked to an AKAP-dependent pool of PKA. This pool would be tightly regulated by spatial compartmentalization of the dopamine receptor, Rut AC, PKA, Dnc, and AKAP. The Dnc gene generates different isoforms (Qiu and Davis, 1993), each of which is characterized by a unique N-terminal region. Long forms of Dnc carry an N-terminal motif that has been highly conserved through evolution (Conti and Beavo, 2007) and has been implicated in binding to AKAPs (Dodge et al., 2001). Dnc isoforms that carry this binding motif may be involved in inhibiting the activation of PKA specifically in the MB medial lobes (Figure 8). In contrast, the pool of PKA involved in appetitive memory would be independent of the macromolecular complex formed by AKAPs and Dnc, and therefore octopaminergic signals would not be spatially regulated by PDEs. As the sensitivity and resolution of imaging techniques improve, it may soon be possible to test this hypothesis directly, by examining PKA dynamics in such microdomains during and after conditioning.

EXPERIMENTAL PROCEDURES

Fly Strains

Flies were reared on a 12 hr dark/12 hr light cycle on standard medium and kept at 18°C. To construct the *UAS-AKAR2* strain, the insert from *pcDNA3*-AKAR2 vector was cut out with XbaI and BamH1 restriction enzymes. After purification, the fragment was cloned into the *pUAST* vector. The resulting construct was injected into w^{1118} embryos (BestGene). Ten independent transgenic homozygous lines were established. One line was chosen for this study based on its relatively high *Gal4*-induced AKAR2 expression (data not shown). For functional imaging studies, we used flies carrying the *UAS-AKAR2* transgene along with the MB *Gal4* driver *238Y* (Yang et al., 1995). The rut^{2080} allele is a P element insertion in the *rut* open reading frame (Levin et al., 1992); dnc^1 was originally isolated as a learning mutant in an ethylmethanesulfonate mutagenesis screen (Dudai et al., 1976). The reference wild-type strain was Canton-Special (Canton-S), and all mutant lines were in a Canton-S background.

Behavioral Assays

For all imaging and behavioral experiments, 1- to 3-day-old flies were used. Training and testing were performed at 25°C and at 65%–80% relative humidity, as previously described for aversive memory and appetitive memory (Pascual and Preat, 2001; Colomb et al., 2009).

Live Imaging

Preparation of flies for live imaging was performed as previously described (Fiala and Spall, 2003). Untrained flies were removed from culture bottles and glued to a plastic coverslip coated with a thin transparent plastic sheet. The coverslip was then placed on the recording chamber. A drop of *Drosophila* Ringer's solution was placed over the head (130 mM NaCl, 5 mM KCl, 2 mM MgCl$_2$, 2 mM CaCl$_2$, 36 mM sucrose, 5 mM HEPES-NaOH [pH 7.3]). A small region of cuticle was cut away from the top of the head capsule, and trachea were removed from the area. Flies were then placed under a Leica DM6000 microscope and observed with a 20× water-immersion objective (NA = 1; Leica). Experiments were performed at room temperature. Brains were continuously perfused with *Drosophila* Ringer's solution. Stocks of forskolin and IBMX were dissolved in DMSO and subsequently diluted (1/1000) in *Drosophila* Ringer's solution before being applied to the fly brain by bath application. All chemicals (forskolin, IBMX, dopamine, octopamine, acetylcholine, TTX) were purchased from Sigma except Rp-8-CPT-cAMPs (Biolog).

Two-photon excitation was obtained with a mode-locked Ti:sapphire laser (Chameleon Ultra; Coherent). The AKAR2 FRET probe contains CFP and a YFP variant named citrine (Zhang et al., 2005). The excitation spectra of CFP and YFP have already been described (Zipfel et al., 2003), and a relatively specific excitation of CFP over YFP is obtained at 820 nm. We verified the specificity of this excitation using *UAS-CFP* and *UAS-YFP Drosophila* strains to express CFP and YFP in MB neurons. Emitted light passed through a short-pass SP700 filter and was then split by a dichroic mirror at 506 nm (Semrock) and filtered through band-pass filters (CFP: peak 483 nm, bandwidth 32 nm [Semrock]; citrine: peak 542 nm, bandwidth 27 nm [Semrock]). Scanning and acquisition were controlled by LAS AF software (Leica). We measured CFP photobleaching by acquisition of AKAR2 fluorescence during 2 hr without stimulation, and no significant decrease in fluorescence intensity was detected in the CFP channel. To determine levels of YFP photobleaching, we took advantage of the specific excitation of YFP at 970 nm and acquired one image at 970 nm at the beginning and at the end of the imaging session. No significant decrease in YFP fluorescence was detected.

Image Analysis

CFP and YFP images (512 × 512 pixels) were acquired simultaneously with a line rate of 400 Hz. Four frames were acquired per minute. To obtain FRET ratio time courses, CFP and YFP images at each time point were background subtracted (background was evaluated as the mean intensity over a region of interest placed in a nonfluorescent part of the brain). YFP or CFP emission intensities for each image were then averaged within a region of interest. These values were used to calculate the yellow/cyan emission ratio, which was then normalized to the ratio before drug application. For emission ratio images, a similar approach was used on a pixel-by-pixel basis using LAS AF (Leica) or Igor software (Wavemetrics). Statistical significance was determined at $p < 0.05$ using one-way ANOVA with Tukey-HSD as the post hoc test. Data are expressed as mean ± SEM.

REFERENCES

Abrams, T.W., and Kandel, E.R. (1988). Is contiguity detection in classical conditioning a system or a cellular property? Learning in *Aplysia* suggests a possible molecular site. Trends Neurosci. *11*, 128–135.

Akalal, D.B., Wilson, C.F., Zong, L., Tanaka, N.K., Ito, K., and Davis, R.L. (2006). Roles for *Drosophila* mushroom body neurons in olfactory learning and memory. Learn. Mem. *13*, 659–668.

Bacskai, B.J., Hochner, B., Mahaut-Smith, M., Adams, S.R., Kaang, B.K., Kandel, E.R., and Tsien, R.Y. (1993). Spatially resolved dynamics of cAMP and protein kinase A subunits in *Aplysia* sensory neurons. Science *260*, 222–226.

Beavo, J.A., and Brunton, L.L. (2002). Cyclic nucleotide research—still expanding after half a century. Nat. Rev. Mol. Cell Biol. *3*, 710–718.

Beavo, J.A., Rogers, N.L., Crofford, O.B., Hardman, J.G., Sutherland, E.W., and Newman, E.V. (1970). Effects of xanthine derivatives on lipolysis and on adenosine 3′,5′-monophosphate phosphodiesterase activity. Mol. Pharmacol. *6*, 597–603.

Blum, A.L., Li, W., Cressy, M., and Dubnau, J. (2009). Short- and long-term memory in *Drosophila* require cAMP signaling in distinct neuron types. Curr. Biol. *19*, 1341–1350.

Busch, S., Selcho, M., Ito, K., and Tanimoto, H. (2009). A map of octopaminergic neurons in the *Drosophila* brain. J. Comp. Neurol. *513*, 643–667.

Byers, D., Davis, R.L., and Kiger, J.A., Jr. (1981). Defect in cyclic AMP phosphodiesterase due to the dunce mutation of learning in *Drosophila melanogaster*. Nature *289*, 79–81.

Claridge-Chang, A., Roorda, R.D., Vrontou, E., Sjulson, L., Li, H., Hirsh, J., and Miesenböck, G. (2009). Writing memories with light-addressable reinforcement circuitry. Cell *139*, 405–415.

Colomb, J., Kaiser, L., Chabaud, M.A., and Preat, T. (2009). Parametric and genetic analysis of *Drosophila* appetitive long-term memory and sugar motivation. Genes Brain Behav. *8*, 407–415.

Connolly, J.B., Roberts, I.J., Armstrong, J.D., Kaiser, K., Forte, M., Tully, T., and O'Kane, C.J. (1996). Associative learning disrupted by impaired Gs signaling in *Drosophila* mushroom bodies. Science *274*, 2104–2107.

Conti, M., and Beavo, J. (2007). Biochemistry and physiology of cyclic nucleotide phosphodiesterases: essential components in cyclic nucleotide signaling. Annu. Rev. Biochem. *76*, 481–511.

Crittenden, J.R., Skoulakis, E.M., Han, K.A., Kalderon, D., and Davis, R.L. (1998). Tripartite mushroom body architecture revealed by antigenic markers. Learn. Mem. *5*, 38–51.

Davis, R.L., and Kiger, J.A., Jr. (1981). dunce mutants of *Drosophila melanogaster*: mutants defective in the cyclic AMP phosphodiesterase enzyme system. J. Cell Biol. *90*, 101–107.

de Belle, J.S., and Heisenberg, M. (1994). Associative odor learning in *Drosophila* abolished by chemical ablation of mushroom bodies. Science *263*, 692–695.

de Souza, N.J., Dohadwalla, A.N., and Reden, J. (1983). Forskolin: a labdane diterpenoid with antihypertensive, positive inotropic, platelet aggregation inhibitory, and adenylate cyclase activating properties. Med. Res. Rev. *3*, 201–219.

Dodge, K.L., Khouangsathiene, S., Kapiloff, M.S., Mouton, R., Hill, E.V., Houslay, M.D., Langeberg, L.K., and Scott, J.D. (2001). mAKAP assembles a protein kinase A/PDE4 phosphodiesterase cAMP signaling module. EMBO J. *20*, 1921–1930.

Dodge-Kafka, K.L., Soughayer, J., Pare, G.C., Carlisle Michel, J.J., Langeberg, L.K., Kapiloff, M.S., and Scott, J.D. (2005). The protein kinase A anchoring protein mAKAP coordinates two integrated cAMP effector pathways. Nature *437*, 574–578.

Drain, P., Folkers, E., and Quinn, W.G. (1991). cAMP-dependent protein kinase and the disruption of learning in transgenic flies. Neuron *6*, 71–82.

Dubnau, J., Grady, L., Kitamoto, T., and Tully, T. (2001). Disruption of neurotransmission in *Drosophila* mushroom body blocks retrieval but not acquisition of memory. Nature *411*, 476–480.

Dudai, Y. (1985). Some properties of adenylate cyclase which might be important for memory formation. FEBS Lett. *191*, 165–170.

Dudai, Y., Jan, Y.N., Byers, D., Quinn, W.G., and Benzer, S. (1976). dunce, a mutant of *Drosophila* deficient in learning. Proc. Natl. Acad. Sci. USA *73*, 1684–1688.

Dunn, T.A., Wang, C.T., Colicos, M.A., Zaccolo, M., DiPilato, L.M., Zhang, J., Tsien, R.Y., and Feller, M.B. (2006). Imaging of cAMP levels and protein kinase A activity reveals that retinal waves drive oscillations in second-messenger cascades. J. Neurosci. *26*, 12807–12815.

Fiala, A., and Spall, T. (2003). In vivo calcium imaging of brain activity in *Drosophila* by transgenic cameleon expression. Sci. STKE *2003*, PL6.

Gerber, B., Tanimoto, H., and Heisenberg, M. (2004). An engram found? Evaluating the evidence from fruit flies. Curr. Opin. Neurobiol. *14*, 737–744.

Gervasi, N., Hepp, R., Tricoire, L., Zhang, J., Lambolez, B., Paupardin-Tritsch, D., and Vincent, P. (2007). Dynamics of protein kinase A signaling at the membrane, in the cytosol, and in the nucleus of neurons in mouse brain slices. J. Neurosci. *27*, 2744–2750.

Gjertsen, B.T., Mellgren, G., Otten, A., Maronde, E., Genieser, H.G., Jastorff, B., Vintermyr, O.K., McKnight, G.S., and Doskeland, S.O. (1995). Novel (Rp)-cAMPS analogs as tools for inhibition of cAMP-kinase in cell culture. Basal cAMP-kinase activity modulates interleukin-1β action. J. Biol. Chem. *270*, 20599–20607.

Han, P.L., Levin, L.R., Reed, R.R., and Davis, R.L. (1992). Preferential expression of the *Drosophila* rutabaga gene in mushroom bodies, neural centers for learning in insects. Neuron *9*, 619–627.

Han, K.A., Millar, N.S., Grotewiel, M.S., and Davis, R.L. (1996). DAMB, a novel dopamine receptor expressed specifically in *Drosophila* mushroom bodies. Neuron *16*, 1127–1135.

Han, K.A., Millar, N.S., and Davis, R.L. (1998). A novel octopamine receptor with preferential expression in *Drosophila* mushroom bodies. J. Neurosci. *18*, 3650–3658.

Heisenberg, M., Borst, A., Wagner, S., and Byers, D. (1985). *Drosophila* mushroom body mutants are deficient in olfactory learning. J. Neurogenet. *2*, 1–30.

Hempel, C.M., Vincent, P., Adams, S.R., Tsien, R.Y., and Selverston, A.I. (1996). Spatio-temporal dynamics of cyclic AMP signals in an intact neural circuit. Nature *384*, 166–169.

Horiuchi, J., Yamazaki, D., Naganos, S., Aigaki, T., and Saitoe, M. (2008). Protein kinase A inhibits a consolidated form of memory in *Drosophila*. Proc. Natl. Acad. Sci. USA *105*, 20976–20981.

Isabel, G., Pascual, A., and Preat, T. (2004). Exclusive consolidated memory phases in *Drosophila*. Science *304*, 1024–1027.

Keene, A.C., and Waddell, S. (2007). *Drosophila* olfactory memory: single genes to complex neural circuits. Nat. Rev. Neurosci. *8*, 341–354.

Kim, Y.C., Lee, H.G., Seong, C.S., and Han, K.A. (2003). Expression of a D1 dopamine receptor dDA1/DmDOP1 in the central nervous system of *Drosophila melanogaster*. Gene Expr. Patterns *3*, 237–245.

Krashes, M.J., and Waddell, S. (2008). Rapid consolidation to a radish and protein synthesis-dependent long-term memory after single-session appetitive olfactory conditioning in *Drosophila*. J. Neurosci. *28*, 3103–3113.

Krashes, M.J., Keene, A.C., Leung, B., Armstrong, J.D., and Waddell, S. (2007). Sequential use of mushroom body neuron subsets during *Drosophila* odor memory processing. Neuron *53*, 103–115.

Krashes, M.J., DasGupta, S., Vreede, A., White, B., Armstrong, J.D., and Waddell, S. (2009). A neural circuit mechanism integrating motivational state with memory expression in *Drosophila*. Cell *139*, 416–427.

Levin, L.R., Han, P.L., Hwang, P.M., Feinstein, P.G., Davis, R.L., and Reed, R.R. (1992). The *Drosophila* learning and memory gene rutabaga encodes a Ca^{2+}/calmodulin-responsive adenylyl cyclase. Cell *68*, 479–489.

Lissandron, V., Rossetto, M.G., Erbguth, K., Fiala, A., Daga, A., and Zaccolo, M. (2007). Transgenic fruit-flies expressing a FRET-based sensor for in vivo imaging of cAMP dynamics. Cell. Signal. *19*, 2296–2303.

Liu, X., and Davis, R.L. (2006). Insect olfactory memory in time and space. Curr. Opin. Neurobiol. *16*, 679–685.

Livingstone, M.S. (1985). Genetic dissection of *Drosophila* adenylate cyclase. Proc. Natl. Acad. Sci. USA *82*, 5992–5996.

Livingstone, M.S., Sziber, P.P., and Quinn, W.G. (1984). Loss of calcium/calmodulin responsiveness in adenylate cyclase of rutabaga, a *Drosophila* learning mutant. Cell *37*, 205–215.

Makos, M.A., Kim, Y.C., Han, K.A., Heien, M.L., and Ewing, A.G. (2009). In vivo electrochemical measurements of exogenously applied dopamine in Drosophila melanogaster. Anal. Chem. *81*, 1848–1854.

Mank, M., Santos, A.F., Direnberger, S., Mrsic-Flogel, T.D., Hofer, S.B., Stein, V., Hendel, T., Reiff, D.F., Levelt, C., Borst, A., et al. (2008). A genetically

encoded calcium indicator for chronic in vivo two-photon imaging. Nat. Methods *5*, 805–811.

Mao, Z., and Davis, R.L. (2009). Eight different types of dopaminergic neurons innervate the *Drosophila* mushroom body neuropil: anatomical and physiological heterogeneity. Front. Neural Circuits *3*, 5.

McGuire, S.E., Le, P.T., Osborn, A.J., Matsumoto, K., and Davis, R.L. (2003). Spatiotemporal rescue of memory dysfunction in *Drosophila*. Science *302*, 1765–1768.

Narahashi, T., Moore, J.W., and Scott, W.R. (1964). Tetrodotoxin blockage of sodium conductance increase in lobster giant axons. J. Gen. Physiol. *47*, 965–974.

Nassel, D.R., and Elekes, K. (1992). Aminergic neurons in the brain of blowflies and *Drosophila*: dopamine- and tyrosine hydroxylase-immunoreactive neurons and their relationship with putative histaminergic neurons. Cell Tissue Res. *267*, 147–167.

Neves, S.R., Tsokas, P., Sarkar, A., Grace, E.A., Rangamani, P., Taubenfeld, S.M., Alberini, C.M., Schaff, J.C., Blitzer, R.D., Moraru, I.I., and Iyengar, R. (2008). Cell shape and negative links in regulatory motifs together control spatial information flow in signaling networks. Cell *133*, 666–680.

Nighorn, A., Healy, M.J., and Davis, R.L. (1991). The cyclic AMP phosphodiesterase encoded by the *Drosophila* dunce gene is concentrated in the mushroom body neuropil. Neuron *6*, 455–467.

Nikolaev, V.O., Bunemann, M., Hein, L., Hannawacker, A., and Lohse, M.J. (2004). Novel single chain cAMP sensors for receptor-induced signal propagation. J. Biol. Chem. *279*, 37215–37218.

Pascual, A., and Preat, T. (2001). Localization of long-term memory within the *Drosophila* mushroom body. Science *294*, 1115–1117.

Qiu, Y., and Davis, R.L. (1993). Genetic dissection of the learning/memory gene dunce of *Drosophila melanogaster*. Genes Dev. *7*, 1447–1458.

Riemensperger, T., Voller, T., Stock, P., Buchner, E., and Fiala, A. (2005). Punishment prediction by dopaminergic neurons in *Drosophila*. Curr. Biol. *15*, 1953–1960.

Saucerman, J.J., Brunton, L.L., Michailova, A.P., and McCulloch, A.D. (2003). Modeling β-adrenergic control of cardiac myocyte contractility in silico. J. Biol. Chem. *278*, 47997–48003.

Saucerman, J.J., Zhang, J., Martin, J.C., Peng, L.X., Stenbit, A.E., Tsien, R.Y., and McCulloch, A.D. (2006). Systems analysis of PKA-mediated phosphorylation gradients in live cardiac myocytes. Proc. Natl. Acad. Sci. USA *103*, 12923–12928.

Schroll, C., Riemensperger, T., Bucher, D., Ehmer, J., Voller, T., Erbguth, K., Gerber, B., Hendel, T., Nagel, G., Buchner, E., and Fiala, A. (2006). Light-induced activation of distinct modulatory neurons triggers appetitive or aversive learning in *Drosophila* larvae. Curr. Biol. *16*, 1741–1747.

Schwaerzel, M., Monastirioti, M., Scholz, H., Friggi-Grelin, F., Birman, S., and Heisenberg, M. (2003). Dopamine and octopamine differentiate between aversive and appetitive olfactory memories in *Drosophila*. J. Neurosci. *23*, 10495–10502.

Schwaerzel, M., Jaeckel, A., and Mueller, U. (2007). Signaling at A-kinase anchoring proteins organizes anesthesia-sensitive memory in *Drosophila*. J. Neurosci. *27*, 1229–1233.

Shafer, O.T., Kim, D.J., Dunbar-Yaffe, R., Nikolaev, V.O., Lohse, M.J., and Taghert, P.H. (2008). Widespread receptivity to neuropeptide PDF throughout the neuronal circadian clock network of *Drosophila* revealed by real-time cyclic AMP imaging. Neuron *58*, 223–237.

Sinakevitch, I., and Strausfeld, N.J. (2006). Comparison of octopamine-like immunoreactivity in the brains of the fruit fly and blow fly. J. Comp. Neurol. *494*, 460–475.

Skoulakis, E.M., Kalderon, D., and Davis, R.L. (1993). Preferential expression in mushroom bodies of the catalytic subunit of protein kinase A and its role in learning and memory. Neuron *11*, 197–208.

Tanaka, N.K., Tanimoto, H., and Ito, K. (2008). Neuronal assemblies of the *Drosophila* mushroom body. J. Comp. Neurol. *508*, 711–755.

Taylor, S.S., Buechler, J.A., and Yonemoto, W. (1990). cAMP-dependent protein kinase: framework for a diverse family of regulatory enzymes. Annu. Rev. Biochem. *59*, 971–1005.

Tempel, B.L., Bonini, N., Dawson, D.R., and Quinn, W.G. (1983). Reward learning in normal and mutant *Drosophila*. Proc. Natl. Acad. Sci. USA *80*, 1482–1486.

Thum, A.S., Jenett, A., Ito, K., Heisenberg, M., and Tanimoto, H. (2007). Multiple memory traces for olfactory reward learning in *Drosophila*. J. Neurosci. *27*, 11132–11138.

Tomchik, S.M., and Davis, R.L. (2009). Dynamics of learning-related cAMP signaling and stimulus integration in the *Drosophila* olfactory pathway. Neuron *64*, 510–521.

Tully, T., and Quinn, W.G. (1985). Classical conditioning and retention in normal and mutant *Drosophila melanogaster*. J. Comp. Physiol. [A] *157*, 263–277.

Tully, T., Preat, T., Boynton, S.C., and Del Vecchio, M. (1994). Genetic dissection of consolidated memory in *Drosophila*. Cell *79*, 35–47.

Vincent, P., Gervasi, N., and Zhang, J. (2008). Real-time monitoring of cyclic nucleotide signaling in neurons using genetically encoded FRET probes. Brain Cell Biol. *36*, 3–17.

Wang, Y., Mamiya, A., Chiang, A.S., and Zhong, Y. (2008). Imaging of an early memory trace in the *Drosophila* mushroom body. J. Neurosci. *28*, 4368–4376.

Wong, W., and Scott, J.D. (2004). AKAP signalling complexes: focal points in space and time. Nat. Rev. Mol. Cell Biol. *5*, 959–970.

Wu, Z.L., Thomas, S.A., Villacres, E.C., Xia, Z., Simmons, M.L., Chavkin, C., Palmiter, R.D., and Storm, D.R. (1995). Altered behavior and long-term potentiation in type I adenylyl cyclase mutant mice. Proc. Natl. Acad. Sci. USA *92*, 220–224.

Yamazaki, D., Horiuchi, J., Nakagami, Y., Nagano, S., Tamura, T., and Saitoe, M. (2007). The *Drosophila* DCO mutation suppresses age-related memory impairment without affecting lifespan. Nat. Neurosci. *10*, 478–484.

Yang, M.Y., Armstrong, J.D., Vilinsky, I., Strausfeld, N.J., and Kaiser, K. (1995). Subdivision of the *Drosophila* mushroom bodies by enhancer-trap expression patterns. Neuron *15*, 45–54.

Yin, J.C., Wallach, J.S., Del Vecchio, M., Wilder, E.L., Zhou, H., Quinn, W.G., and Tully, T. (1994). Induction of a dominant negative CREB transgene specifically blocks long-term memory in *Drosophila*. Cell *79*, 49–58.

Yu, D., Keene, A.C., Srivatsan, A., Waddell, S., and Davis, R.L. (2005). *Drosophila* DPM neurons form a delayed and branch-specific memory trace after olfactory classical conditioning. Cell *123*, 945–957.

Yu, D., Akalal, D.B., and Davis, R.L. (2006). *Drosophila* α/β mushroom body neurons form a branch-specific, long-term cellular memory trace after spaced olfactory conditioning. Neuron *52*, 845–855.

Zars, T., Fischer, M., Schulz, R., and Heisenberg, M. (2000). Localization of a short-term memory in *Drosophila*. Science *288*, 672–675.

Zhang, J., Ma, Y., Taylor, S.S., and Tsien, R.Y. (2001). Genetically encoded reporters of protein kinase A activity reveal impact of substrate tethering. Proc. Natl. Acad. Sci. USA *98*, 14997–15002.

Zhang, J., Hupfeld, C.J., Taylor, S.S., Olefsky, J.M., and Tsien, R.Y. (2005). Insulin disrupts β-adrenergic signalling to protein kinase A in adipocytes. Nature *437*, 569–573.

Zhong, Y., and Wu, C.F. (1991). Altered synaptic plasticity in *Drosophila* memory mutants with a defective cyclic AMP cascade. Science *251*, 198–201.

Zhong, Y., and Wu, C.F. (2004). Neuronal activity and adenylyl cyclase in environment-dependent plasticity of axonal outgrowth in *Drosophila*. J. Neurosci. *24*, 1439–1445.

Zipfel, W.R., Williams, R.M., and Webb, W.W. (2003). Nonlinear magic: multiphoton microscopy in the biosciences. Nat. Biotechnol. *21*, 1369–1377.